Accepted Manuscript

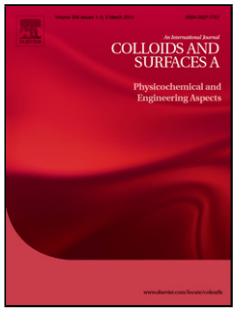

Title: Preparation and structure's analyses of lanthanide (Ln) -exchanged bentonites

Authors: Eszter Mária Kovács, Eszter Erdélyiné Baradács, Péter Kónya, Péter Kovács-Pálffy, Sándor Harangi, József Kónya, Noémi M. Nagy

PII: S0927-7757(17)30219-4
DOI: http://dx.doi.org/doi:10.1016/j.colsurfa.2017.02.085
Reference: COLSUA 21440

To appear in: *Colloids and Surfaces A: Physicochem. Eng. Aspects*

Received date: 11-1-2017
Revised date: 24-2-2017
Accepted date: 27-2-2017

Please cite this article as: Eszter Mária Kovács, Eszter Erdélyiné Baradács, Péter Kónya, Péter Kovács-Pálffy, Sándor Harangi, József Kónya, Noémi M.Nagy, Preparation and structure's analyses of lanthanide (Ln) -exchanged bentonites, Colloids and Surfaces A: Physicochemical and Engineering Aspects http://dx.doi.org/10.1016/j.colsurfa.2017.02.085

Preparation and structure's analyses of lanthanide (Ln) -exchanged bentonites

Eszter Mária Kovács[1], Eszter Erdélyiné Baradács[2], Péter Kónya[3], Péter Kovács-Pálffy[3], Sándor Harangi[4], József Kónya[1], and Noémi M. Nagy [1*]

[1]*Imre Lajos Isotope Laboratory, Department of Colloid and Environmental Chemistry, University of Debrecen, Debrecen, 4032 Egyetem tér 1., Hungary*

[2]*Department of Solid State Physics, University of Debrecen, Debrecen, 4026 Bem tér 18/b, Hungary*

[3]*Geological and Geophysical Institute of Hungary, H-1143 Hungary*

[4]*Department of Inorganic and Analytical Chemistry, Agilent Atomic Spectroscopy Partner Laboratory, University of Debrecen, H-4032 Debrecen, Hungary*

**Corresponding author: nagy.noemi@science.unideb.hu*

GRAPHICAL ABSTRACTS

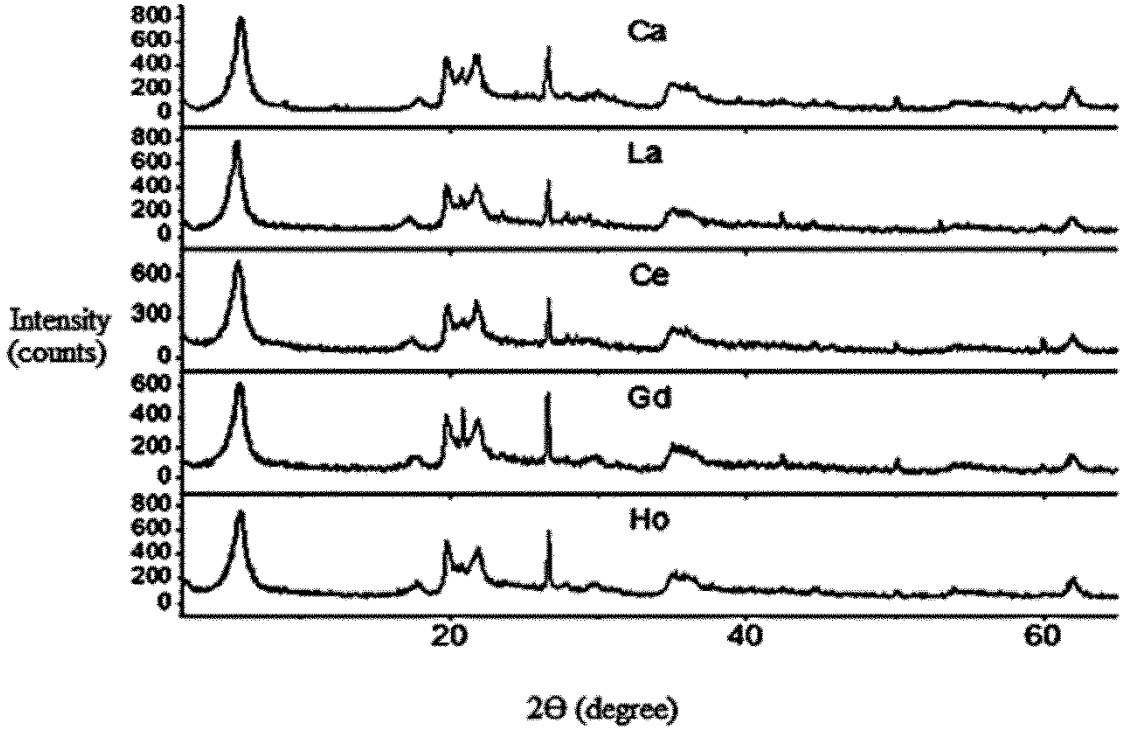

X-ray diffractograms of lathanide cation exchanged benonites

HIGHLIGHTS

- REE-exchanged bentonites were prepared from Ca-bentonite by ion exchange.
- The La^{3+}-, Ce^{3+}-, and Gd^{3+}-bentonite, the sorbed ion amount was higher than the CEC.
- In case of lanthanum-bentonite, the rare earth quantity is as high as 136% of CEC.
- The iron(III) content of lanthanum bentonite is less than that of the original Ca-bentonite.

Abstract The interaction between **Lanthanides (Ln)**- ions and Ca-bentonite and the structural changes accompanying were studied. **Ln**-exchanged bentonites were prepared from Ca-bentonite (Istenmezeje, Hungary) by ion exchange in three consecutive washings with **lanthanide** solutions. Scanning Eletronmicroscopy Energy Dispersive X-ray spectroscopy (SEM-EDX) studies showed even distribution of **Ln**s and other components of bentonite. The natural bentonite and the lanthnide exchanged bentonites were characterized by X-ray diffraction (XRD), which revealed the same mineral composition, and the increase of the basal spacing of montmorillonite from 1.465 (Ca^{2+}) to 1.577 nm (REE^{3+}). The d_{001} basal spacing of **lanthanide** montmorillonite increases as the ion radius of the **lanthanide** cation increases. The Fe^{3+}, and **Ln**s^{3+} amount on the bentonite were determined by X-ray-fluorescence spectrometry (XRF) elemental analysis. The amount of exchanged **Ln**s were determined by washing the **Ln**-bentonite with 1M ammonium-acetate, and measuring the amount of **Ln** released, using inductively coupled plasma optical emission spectrometry (ICP-OES). In most **Ln**-bentonites, the quantity of the exchanged **Ln** ions was about 80-90% of the cation exchange capacity (CEC) of the bentonite. In case of some **lanthanides** bentonite (La^{3+}, Ce^{3+}, and Gd^{3+}), however, the sorbed quantity of lanthanum ions was higher than the cation exchange capacity. In case of lanthanum-bentonite, the **lanthanide** quantity is as high as 136% of CEC. Moreover, the iron(III) content of lanthanum bentonite is less than that of the original Ca-bentonite. Mössbauer spectra of the La-, Ce-, and Gd-exchanged samples at 78 K revealed an unexpected magnetically split component that was absent from the Ca-bentonite. This component may belong to interlayer Fe. This iron can be released from the octahedral positions crystal lattice.

Keywords: **Ln**-bentonites, Complexometric titration, Scanning electron microscopy, X-ray diffraction, X-ray-fluorescence spectrometry, Inductively Coupled Plasma Optical Emission Spectrometry

1. INTRODUCTION

Structure analyses of bentonites have high interest for industrial and environmental applications [1, 2, 3, 4, 5, 6]. The main mineral of the bentonite is the layer silicate montmorillonite, which has a permanent negative charge because of isomorphic substitutions in the silicate lattice. The negative charge is neutralized by cations attracted to the interlayer space, which space becomes a "nano laboratory" where cation exchange takes place and sometimes modifies the properties of the bentonite.

The natural interlayer cations (mainly sodium and calcium) may be exchanged by **lanthanides** ions. **Lanthanide** ions, can be applied as geological indicators. They will indicate the origin of the rock, differentiation of the origin magma, extraction of certain minerals and the rate of the chemical weathering [7, 8]. Moreover, **lanthanide** ions model interactions between soil and transuranium ions or **lanthanide** cations produced during the fission of ^{235}U in nuclear power plants [9].

A source of **lanthanide** cations is the relatively abundant **lanthanide** ores in a concentration between about 150 to 220 ppm [10] in the Earth's crust [11, 12, 13, 14, 15].

Recent papers on the chemically modified bentonites (Table 1) give a good overview of theirs industrial applications. Coppin et al. [16] studied the complete **lanthanide** series sorption on kaolinite and Na-montmorillonite. They mentioned that the **Ln** sorption is controlled by the nature of the clay minerals, the pH and the ionic strength. The conclusion was that the heavy **Ln**s are being more sorbed than the light **Ln**s at high ionic strength, because of the formation of inner-sphere complexes. Tertre et al. [17] studied the sorption of Eu(III) onto kaolinite and montmorillonite. At the studied temperature, adsorption is the sole process of Eu(III) retention. They identified a unique inner-sphere complex linked to the

aluminol sites in both clays at the edge of the particles (at higher pH), and a second exchangeable outer-sphere complex for montmorillonite, in an interlayer position (under acidic condition). The nature of these complexes does not change with temperature. Stefani et al. [18] studied the lanthanum-saturated montmorillonite under high pressure and high temperature. Under these conditions the structure becomes muscovite-like and rich in La^{3+}. Wu et al. [19] synthesized magnetic bentonite to adsorb **lanthanide** ions. They used it to remove **lanthanide** ions from aqueous solution. The adsorption is less efficient on magnetic bentonite than on the original bentonite in removing **lanthanide** ions. Evgeny et al. [20] incubated FEBEX and MX80 bentonites in the presence of Fe(0) which formed crystalline goethite in the structure. **Lanthanides** are sorbed on smectite, and also at the Fe oxide phases. The increase of the **lanthanides** sorption was overcame by the smectite degradation induced by the presence of Fe.

In these studies, the authors used **Ln**s in low concentration, so the **Ln** ions intercalated into the interlayer of smectite cannot change the clay. The works cited deal with some specific **Ln** cations.

Table 1

In this work, the preparation and properties of all **Ln** (La, Ce, Pr, Nd, Sm, Eu, Gd, Tb, Dy, Ho, Er, Tm, Yb and Lu) modified bentonites (except the radioactive promethium) will be discussed. **Ln**s are used in high concentration, and **Ln**-bentonites are produced by three cation exchange processes. The structure of these **Ln**-bentonites is studied by XRD, XRF, SEM-EDX, complexometric titration, ICP-OES and Mössbauer-spectroscopy. The results can prove the suggestion by Coppin et al. [16], Wu et al. [19], and Tertre et al. [17] on the intercalation of **Ln** ions in the interlayer of smectite. In addition, information will be shown on the structural parameters of trivalent **lanthanide** cation exchanged bentonites.

Furthermore, a surprising information studied about the structural Fe, which is oppose to the studies of Evgeny et al. [20], and Stefani et al. [18] that during cation exchange procedure no other crystalline phase formed but octahedral Fe may moves into interlayer phase.

2. EXPERIMENTAL

2.1 Characterization of Ca-bentonite

The Ca-bentonite starting material was obtained from Istenmezeje, Hungary, and was characterized with respect to its mineralogy and cation exchange capacity (CEC). Elemental analysis of the original Ca-bentonite resulted in the following composition: 73.29 % SiO_2, 18.71 % Al_2O_3, 2.98 % Fe-oxide, 1.54 % CaO and 3.48 % MgO. The mineral composition was determined by means of X-ray powder diffraction (XRD) analysis the use of Philips PW1710 diffractometer (Philips, (today PANalytical B.V.) De Schakel 18 5651 GH Eindhoven, Netherland), which is operating at 30 mA and 40 kV using Cu Kα radiation source and a graphite monochromator. The scanning rate was 2°2θ/min. The mineral composition was calculated on the basis of the relative intensities of the reflections characteristic of the minerals, applying the literature or experimental corundum factors on minerals [21, 22, 23, 24].

Further differentiation of mineralogy was accomplished previously by Kónya et al. [25] using derivatograph-PC, a computer-controlled simultaneous TG, DTG, DTA apparatus (MOM Szerviz KFT, Budapest, Hungary) ,and only the results are shown in this section. Measurement conditions were: 10°C min–1 heating rate, air atmosphere, ceramic crucible, mass sample about 100 mg, reference material Al_2O_3 temperature 25-1000 °C. The measurement by X-ray diffraction (intensity of the basal reflection) and thermoanalytical (based on mass loss upon heating) show 71 % montmorillonite content. The other constituents were: 12 m/m% cristobalite, opal CT, 8 m/m% illite, 4 m/m% quartz, 3 m/m%

kaolinite, and 2 m/m% calcite. The basal space d_{001} of montmorillonite was 1.465 nm showing the dioctahedral character of the smectites.

The CEC, as determined by the ammonium acetate method [26], was 81 mmol/100 g for monovalent cations.

*2.2 Preparation of **Ln**-bentonites*

The **Ln**-bentonites were prepared from the starting bentonite material described above and from **Ln**-oxides as follows. The oxides of **Ln**s (La, Ce, Pr, Nd, Sm, Eu, Gd, Tb, Dy, Ho, Er, Tm, Yb, and Lu) were dissolved in concentrated HCl resulting LnCls and the excess HCl was evaporated at 80°C for about 2 h 35 mins on a heating plate. The remained chlorides of **Ln**s in the bottom of the beaker were dissolved in water. **Ln**s were precipitated in their carbonate forms using ammonium carbonate. After filtering, the **Ln**-carbonates were dissolved in a known amount of 0.1 mol dm^{-3} $HClO_4$ to produce a stock solution (~50 cm^3, pH=5-5.5, ~ 0.1 mol dm^{-3}) for use in the cation exchange procedure described below. This **Ln**-perchlorate solution (~ 50 cm^3, pH=5-5.5, ~ 0.1 mol dm^{-3}) was used in the ion-exchange procedure. The **Ln** concentration was measured by complexometric titration.

Ln-bentonites were produced by suspending 2 g Ca-bentonite starting material in 20 cm^3 of the **Ln**-perchlorate solution prepared above. The suspension was stirred for 5 h at room temperature (25°C), then the supernatant was decanted and saved for elemental analysis, and the cycle started again. Altogether, the ion exchange procedure was carried out 3 times. At the end of the preparation, the **Ln**-bentonites were washed with tridistilled water, then air-dried.

To check some surprising results, lanthanum-bentonite was prepared at different concentration of the **Ln** perchlorate solution (0.1-0.2 $moldm^{-3}$) and temperatures (0°, 10°, 25°, 30°, 40°C).

2.3 Complexometric titration

Supernatants collected during the cation exchange procedure above were analyzed for Ca and **Ln** cations using complexometric titration. Briefly, these cations were titrated with ethylenediamintetraacetic acid (EDTA), using murexid and xilenolorange, respectively, as indicators [27].

The complex formation of Ca^{2+} and EDTA can be expressed as follows:

$$Ca^{2+} + EDTA^{4-} = [CaEDTA]^{2-} \quad \text{(Eq.(1))}$$

murexid with Ca^{2+} gives pink dye complex; when Ca^{2+} runs out pink color will become purple between pH 12-13.

Complex formation of **Ln**s and EDTA can be expressed as follows:

$$\boldsymbol{Ln}^{3+} + EDTA^{4-} = [\boldsymbol{Ln}EDTA]^{-} \quad \text{(Eq.(2))}$$

xilenolorange with $\mathbf{Ln}^{3+}$s gives purple dye complex; when $\mathbf{Ln}^{3+}$s runs out purple colour become yellow between pH 5.8-6.

The concentration of Ca and **Ln**s were calculated with Eq.(3)

$$c_1 = \frac{c_2 * V_2}{V_1}, \quad \text{(Eq.(3))}$$

where c_1 [moldm^{-3}] is the concentration of Ca or **Ln**s, V_1 is the titrated supernatants [cm^3], c_2 is the concentration of EDTA [moldm^{-3}] and V_2 is the consumed EDTA [cm^3].

2.4 XRF measurements

Elemental analysis of the **Ln**-bentonites in the solid state was carried out using energy dispersive X-ray fluorescence spectroscopy. Instrumental parameters were:

1. Si(Li) detector with 20 mm^2 surface and 3.5 mm evaporated layer (Atomki, Debrecen, Hungary),

2. Canberra DSA 1000 digital spectrum analyzer (Camberra Industries, Meriden, CT 06450, USA),
3. Canberra Genie 2000 3.0 spectroscopy software (Camberra Industries, Meriden, CT 06450, USA).

The K_α-lines of the **lanthanide** elements can be excited with 185 MBq ^{241}Am radioactive source, except Yb and Lu. These two elements require a higher energy than the ^{241}Am K_α-line (60 keV) radioactive source, so they were measured using the L_α- and L_β-lines, respectively. In addition to the **lanthanide**s, samples were also analyzed for iron (Fe) using the K_α-lines of a tungsten X-ray tube (type: S6000, Oxford Instruments, Scotts Valley, CA 95066, USA), operating at 60 kV and 1 mA.

2.5 SEM measurements

Scanning electron microscopy (SEM) images were obtained using a Hitachi S4300 CFE electron microscope (Europark Fichtenhain A12 47807 Krefeld Germany) and elemental maps were measured using a BRUKER Quantax XFlash SEM (Bruker Nano GmbH Am Studio 2D 12489 Berlin Germany) with a 4 SSD (Silicon Drift Detector) X-ray detector.

Samples were powdered in an agate mortar, sprinkled on two-sided glue which was put onto the sample holder.

2.6 XRD measurements

XRD diffractograms of natural Ca-benonite and modified **Ln**-benonites were also recorded using a Philips PW1710 powder diffractometer equipped with a CuK_α source and a graphite monochromator (operating at 30mA, 40kV). The scan rate was 2°2Θ/min. Samples were measured three times using two diffractometers with same parameters involving three scientists.

2.7 Mössbauer spectroscopy measurements

The oxidation state and coordination environment of Fe were determined by Mössbauer spectroscopy, as described by Kuzmann *et al.* [28]. **^{57}Fe Mössbauer measurements were performed in transmission geometry at 78 K and 298 K using a JANIS He cryostat and 20 mCi activity 57Co/Rh sources. The isomer shifts are given relatively to α-Fe. The Mössbauer spectra were evaluated by least-square fitting using the MOSSWINN program.**

2.8 Inductively coupled plasma optical emission spectrometry (ICP-OES) measurements

200 mg of Ca-bentonite and **Ln**-bentonites were suspended in 20 cm^3 of 1M ammonium acetate. The suspension was stirred for 3 h at room temperature (25°C), then supernatants were filtered each time and measured by ICP-OES (Agilent ICP-OES 5100 SVDV, Australia, Melbourne) for Fe, Ca and **Ln**s. Altogether, the washing procedure was carried out 3 times. At the end of the washings, the ammonium acetate washed samples were air-dried, and analyzed for Fe, and **Ln**s by XRF.

2.8.1 Looking for the missing Fe

After the lanthanum cation exchange and measuring the modified samples, an interesting result were recorded (session 3.2): the modification of bentonite reduced the Fe content. A question arised, "where can Fe^{3+} be?". To answer this question, supernatants (solution phases) after the ion exchange processes were refilled in other sample holders then the original sample holders were washed by 20 cm^3 0.004 M HCl. The washing solution (HCl) was chosen to solve the Fe^{3+}, if it is in FeO-OH form on the wall of the sample holder. 1 cm^3 washing solutions were dried at room temperature (25°C) in a plastic sample holder with a

thin plastic foil on the bottom. After a few days, the dried liquid phases were measured for Fe by XRF.

3. RESULTS AND DISCUSSION

3.1 Results of complexometric titration

The progress of ion exchange to produce **Ln**-bentonites through three consecutive washing steps with 0.10 moldm^{-3} **Ln**$^{3+}$ solution was monitored by complexometric titration of the supernatant liquid phase following each washing step. The concentration of Ca^{2+} in the supernatant solutions was high after the first and second washings, but was low after the third washing. From the concentration of the supernatant solutions, we calculated the calcium quantity leaving bentonite and at the same **time** the calcium quantity of bentonite remaining after each exchange (Table 2). After the 1st exchange, 7.7% of the calcium content of the Ca-bentonite starting material remains on bentonite (a mean value for all prepared REE-bentonites which were very similar), this value is 0.6 and 0.05 %, respectively, are after the 2nd and 3rd exchanges. More washes were not needed because after the third wash as low as 0.05% of the Ca content remained on bentonite.

Table 2

3.2 Results of XRF measurements

The REE content of the **Ln**-exchanged bentonites measured by XRF (Table 3).

Table 3

Many (8) **Ln** cations (Table 3) failed to saturate completely the cation exchange capacity of the bentonite, the lowest value is 77% of CEC for Er. The sorption of some light **lanthanide** cations, such as La, Ce, and Gd, however, exceeded the CEC by as much as 136%. To check this high sorption, experiments were carried out with La^{3+}: the cation exchange process was repeated under seven different conditions where the temperature and the initial concentration

of La^{3+}-ion differed. The results show that the sorbed lanthanum quantity increases as the initial lanthanum concentration of the solution and the temperature increases. At the highest concentration and temperature, as high as 136 % of CEC is obtained suggesting the formation of new sorbed species at elevated temperature (Table 3).

At the same time, the iron content of lanthanum exchanged bentonites was determined by XRF (Table 4). We found that Fe concentration was decreased after the exchange with lanthanum ions compared to the Fe content of the Ca-bentonite starting material.

Table 4

The fate of iron during the lanthanum cation exchange will be discussed in session 3.6.

3.3 Results of SEM

In the SEM-EDX spectrum of La-bentonite (Figure 1), the lack of peaks characteristic of Ca and the appearance of La peaks strongly indicate that all Ca has undergone exchange by La.

Similar results were also obtained in case of Ce and Gd -bentonites, indicating successful cation exchange, but for the rest of **Ln** benonites 0.09 atomic% of Ca^{2+} have remained in the structure.

Figure 1 [28]

Elemental distribution maps obtained by SEM-EDX showed the homogeneous distribution of the **lanthanide** ions in these bentonites (Figure 2). The detection limit of this method is about 1000 ppm, which is 0.1 wt%, and this is the minimum amount which is measurable. Standard deviations (RSD) were within acceptable limits for quantitative EDX analysis (< 12 %). The method was used to see the elemental distribution map only in case of **Ln**s and Fe, but at the same time the method was able to analyze quantitatively also. In this

way, we could compare the results of both method (XRF and SEM) characterizing the **Ln** and Fe concentration of bentonites.

Figure 2

3.3.1 The comparison of SEM and XRF concentration results

Lanthanide concentration values measured by SEM-EDX and XRF are compared for selected samples (Table 5). La-, Ce-, and Gd-bentonites were chosen for SEM measurement because of higher sorption than CEC, and Lu-bentonite because the quantity of the exchanged ions was similar to the other **Ln**-bentonites.

Table 5 [28]

The **lanthanide** ion concentrations are near or sometimes higher than cation exchange capacity (2.7×10^{-4} mol/g for trivalent ion) except Lu exchange bentonite (see also Table 2). These two analytical methods gives similar quantitative information within the error limit (±2%).

The slight differences between the **lanthanide** content measured by the two methods can be attributed that SEM-EDX studies the surface while XRF provides information on the bulk. The extreme high concentration data exceeding CEC indicate that **lanthanide** cations can be also incorporated at sites different from those which are in the interlayer space (cation exchange sites).

3.4 Results of XRD

XRD patterns of original Ca-bentonite and selected **Ln**-bentonites are depicted (Figure 3). The diffraction patterns of all **lanthanide** substituted bentonites are quite similar to each other, reflecting that no essential changes occur in the crystal structure and in mineral

composition upon the **lanthanide**s incorporation in the bentonite. This result is consistent with that reported previously for the La-substitution [18].

Figure 3 [28]

In the same time, the differences observed in the corresponding peak positions in the XRD patterns of **Ln**-montmorillonites indicated a change in the d_{001} basal spacing with different **lanthanides** (Figure 4). The difference in the basal spacing between La and Ca montmorillonites is similar to (even somewhat higher) that reported in Stefani *et al.* [18]. Trivalent **lanthanide** ions' basal spacing d_{001} is bigger than with divalent calcium ion (Figure 4); the REE^{3+}-montmorillonite samples were measured three times within an acceptable error limit (±20%).

Figure 4

The d_{001} basal spacing decreases from La (1.577 nm) to Lu (1.479 nm) (Figure 4). The increase of d_{001} basal spacing of **lanthanide** montmorillonites compared to that of Ca-montmorillonite indicates the successful incorporation of **lanthanide** cations into the interlayer space and confirm the successful cation exchange, but it does not say how complete it was.

3.5 Results of Mössbauer spectroscopy studies

As mentioned earlier in session 3.2, there are some $\mathbf{Ln}^{3+}$-ions (La, Ce, Gd) which are sorbed in a higher degree than CEC (Table 3). This observation suggests that these **lanthanide** ions may be also bounded in other sites than montmorillonites interlayer. The question arises: 'What kind of other sites can be present in bentonite?'. A possibility can be that the octahedral iron atoms move into the interlayer space, leaving place for the accommodation of **lanthanide** ions. This idea is an agreement with our previous work [28,

29] where we observed that during the formation of **lanthanide**-bentonites some of the octahedral iron ions moves into the interlayer space, thus providing an empty spot in the crystal lattice which can accommodate **lanthanide** ions.

Figure 5

In fig. 5 the ^{57}Fe Mössbauer spectra of original Ca-bentonite (on the right) and the modified La-bentonite (on the left) were shown which were measured at 78K. The 78 K Mössbauer spectrum (Fig. 5, right side) of original Ca-bentonite is consisting of the two doublets. Unexpectedly, the appearance of a magnetically split component was observed in the Mössbauer spectra of some lanthanide montmorillonites recorded at liquid nitrogen temperature. Figure 5 (on the left) illustrates the sextet component which presents in the 78K spectrum of La exchanged bentonite.

3.6 Results of Inductively coupled plasma optical emission spectrometry studies

Natural Ca-bentonite and La-bentonites were washed by ammonium acetate, and the supernatants were measures by ICP-OES for La and Fe. **Ammonium acetate was chosen to wash the iron supposed from the interlayer phase, thus, the arised question about iron would be answered.** After the washing, solid phases were also measured by XRF for Fe, and La (Table 6).

Ammonium acetate practically washes out the lanthanum from the bentonite. The mass balance shows 5%, and 11 % differences, respectively, for the two samples (7.2e-5 and 7.6e-5 mol, and 5.6e-5 and 5.0e-5 mols, respectively, (Tables 4 and 6).

Only 1.3 % of the total iron can be washed out by ammonium acetate from natural calcium-bentonite; this quantity can be present in other iron minerals or maybe in the interlayer space. The remaining 98.7 % iron are in the octahedral position of crystal lattice.

After lanthanum cation exchanged, the iron quantity of the solid phase decreased in a high degree (Table 6). At the same time, the iron quantity in the solution during the ammonium acetate washing is only very low (0.4 % of the total iron content or less than detection limit). For this reason, the missing iron had to look for.

As mentioned in session 2.8.1 the sample holder used for the lanthanum ion exchange was analysed and we found the missing iron in the HCl solution by which the sample holder was washed. As shown from the mass balance of iron (Table 7), the sum of the iron content in the lanthanum-bentonite, the liquid of ammonium acetate washing, and the HCl solution washed from the sample holders used for the cation exchange well agree with the total iron content of Ca-bentonite (8.0e-5 and 8.6e-5 mol for the two lanthanum-bentonites, respectively and 8.1e-5 mol for Ca-bentonite). The differences are below 6 %. Considering the complicated chemical procedures, this error can be acceptable.

Table 7

4. CONCLUSION

Lanthanid bentonites were prepared from Ca-bentonite by three consecutive ion exchanges. The successful exchange was proved by complexometric titration, XRD, XRF, and SEM-EDX measurements.

The d_{001} basal spacing of montmorillonite changes during the exchange of divalent calcium ions to trivalent **lanthanide** cations. The ion exchange of divalent cation to trivalent ones leads to an increase in the basal spacing, similarly to other trivalent cations. Thus, the growth of basal spacing confirms the ion-exchange.

Some of the **Ln** ions (La, Ce, Gd) showed extreme values of sorption. For La-bentonite, Mössbauer spectroscopy studies [28] show that during the formation of

lanthanide-bentonites a part of the octahedral iron atoms can move [29] into the interlayer space, leaving place for the accommodation of **lanthanide** ions.

Iron quantiy of lanthanum-bentonite is less than that of Ca-bentonite. During the lanthanum cation exchange process, the missing iron was found on the wall of the supernatant holder.

The conclusion is that lanthanum ions can somehow supersede iron from the octahedral positions of crystal lattice. XRD patters, however, show the montmorillonite structure unchanged. We assume that the departure of positively charged iron ions from the lattice increases the negative layer charge and the cation exchange capacity. This can motivate the enhance sorption of lanthanum. This hypothesis is attempted to prove by molecular dynamic calculations.

5. ACKNOWLEDGMENT

The authors thank to Dr. Clara Dufresne (Canada) for the improvement of English.

We acknowledge the Agilent Technologies and the Novo-Lab Ltd. (Hungary) for providing the ICP-OES 5100.

This work was supported by the EU and co-financed by the European Regional Development [GINOP-2.3.2-15-2016-00008]; the Hungarian National Research, Development, and Innovation Office [NKFIH K 120265].

7. REFERENCES

[1] Murray, H.H., Applied Clay Mineralgy - Occurrances, processing and application of kaolins, bentonites, palygorskite-sepiolite, and common clays, 1st edition, Chapter 6: Bentonite Applications, Elsevier, 2, (2007), pp. 111-130.

[2] Bhart, T.V. and Sridharan, A., Prediction of compressibility data for highly plastic clays using diffuse double-layer theory, Clays Clay Miner. 63 (2015) 30-42.

[3] Vasilyeva, M.A., Gusev, Y.A., Shtyrlin, V.G., Greenbaum, A., Puzenko, A., Ben Ishai, P., and Feldman, Y., Dielectric relaxation of water in clay minerals, Clays Clay Miner. 62 (2014) 62-73.

[4] Nagy, N.M., and Kónya, J., Interfacial Chemistry of rocks and soils, Chapter 2: Interfacial Processes in Geological Systems Studies on Montmorillonite Model Substance, CRC Press, (Taylor and Francis Group), New York, USA, 148, (2009), pp. 83-117.

[5] Kaufhold, S., Grissemann, C., Dohrmann, R., Klinkenberg, M., and Decher, A., Comparison of three small-scale devices for the investigation of the electrical conductivity/resistivity of swelling and other clays, Clays Clay Miner. 62 (2014) 1-12.

[6] Heuser, M., Weber, C., Stanjek, H., Chen, H., Jordan, G., Schmahl, W.W., and Natzeck, C., The interaction between bentonite and water vapor. I: examination of physical and chemical properties, Clays Clay Miner. 62 (2014) 188-202.

[7] McDonough, W.F. and Sun, S.-s.,The composition of the Earth, Chem. Geol. 120 (1995) 223-253.

[8] Moyen, J.-F., High Sr/Y and La/Yb ratios: The meaning of the “adakitic signature”, Lithos 112 (2009) 556–574.

[9] Lesnov, F.P., Rare Earth Elements in Ultramafic and Mafic Rocks and their Minerals: main types of rocks. Rock-forming minerals. Chapter 6: Indicator properties of rare earth elements and their role in studies of genesis of rocks and minerals from mafic-ultramafic complexes, CRC Press, (Taylor and Francis Group), New York, USA, (2010), pp. 513-532.

[10] Long, K.R., Van Gosen, B.S., Foley, N.K and Cordier, D., The Principal Rare Earth Elements Deposits of the United States—A Summary of Domestic Deposits and a Global Perspective, Scientific Investigations Report 2010–5220, U.S. Geological Survey, Reston, Virginia, (2010), pp. 3-14.

[11] Karakaya, M.C., Karakaya, N., and Yavuz, F., Geology and conditions of formation of the zeolite-bearing deposit southeast of Ankara (Central Turkey), Clays Clay Miner. 63 (2015) 85-109.

[12] Christidis, G.E., Shriner, C.M., and Murray, H.H., An integrated methodological approach for source-clay determination of ancient ceramics: the case of Aegina Island, Greece, Clays Clay Miner. 62 (2014) 447-469.

[13] Kadir, S., Kulah, T., Eren, M., Onalgil, N., and Gurel, A., Minerological and geochemical characteristics and genesis of the Guzelyurt alunite-bearing kaolinite deposit within the late Miocene Gordeles Ignimbrite, Central Anatolia, Turkey, Clays Clay Miner. 62 (2014) 477- 499.

[14] Kulah, T., Kadir, S., Gurel, A., Eren, M., and Onalgil, N., Mineralogy, geochemistry, and genesis of mudstones in the upper Miocene Mustafapasa member of the Urgup formation in the Cappadocia Region, Central Anatolia, Turkey, Clays Clay Miner. 62 (2014) 267-285.

[15] Emsley, J., Nature’s building blocks: an a-z guide to the elements, new edition, Oxford University Press Inc., U.S., New York, (2011), Pp. 274-277.

[16] Coppin, F., Berger, G., Bauer, A., Castet, S., and Loubet, M., Sorption of lanthanides on smectite and kaolinite, Chem. Geol. 182 (2002) 57–68.

[17] Tertre, E., Berger, G., Simoni, E., Castet, S., Giffaut, E., Loubet, M., and Catalette, H., Europium retention onto clay minerals from 25° to 150°C: experimental measurements, spectroscopic features and sorption modelling, Geochim. Cosmochim. Acta 70 (2006) 4563–4578.

[18] Stefani, V.F., Conceicao, R.V., Camiel, L.C., and Balzaretti, M.L., Stability of lanthanum-saturated montmorillonite under high pressure and high temperature conditions, Appl. Clay Sci. 102 (2014) 51–59.

[19] Wu, D., Zhu, C., Chen, Y., Zhu, B., Yang, Y., Wang, O., and Ye, W., Preparation, characterization and adsorptive study of rare earth ions using magnetic GMZ bentonite, Appl. Clay Sci. 62–63 (2012) 87–93.

[20] Evgeny, G., Alba, M.D., Santos, M.J., and Vidal, M., Effects of the presence of Fe (0) on the sorption of lanthanum and lutetium mixtures in smectites, Appl. Clay Sci. 65–66 (2012) 162–172.

[21] Klug, H.P. and Alexander, L.E., X-ray Diffraction Procedures Polycrystalline and Amorphous Materials, (John Wiley and Sons), New York – London – Paris, (1954), Pp. 716.

[22] Náray-Szabó, I., Zsoldos, L., and Kálmán, A., Bevezetés a röntgendiffrakciós szerkezet kutatásba, jegyzet (in English: Introduction to the X-ray structural studies, lecture notes). Magyar Kémikusok Egyesülete, Budapest, (1965), pp. 305.

[23] Rischák, G., and Viczián, I.,Agyagásványok bázisreflexióinak intenzitását meghatározó tényezők (in English: Mineralogical factors determining the intensity of basal reflections of

clay minerals). — A Magyar Állami Földtani Intézet Évi Jelentése 1972-ről, Budapest, (1974), pp. 229-256.

[24] Rischák, G., Kőzetek és talajok amorf fázisának közvetlen röntgendiffraktometrikus meghatározása (in English: Direct X-ray diffraction analysis of the amorphous phase in rocks and soils). — A Magyar Állami Földtani Intézet Évi Jelentése 1987-ről, Budapest, (1989), pp. 377-394.

[25] Kónya, J., Nagy, N. M., and Földvári, M., The formation and production of nano and micro particles on clays under environmental-like conditions, J. Therm. Anal. Calorim. 79 (2005) 437-543.

[26] Richards, L.A., Diagnosis and Improvement of Saline and Alkaline Soils. - U.S. Department of Agriculture, (Soil and Water Conservation Research Branch, Agricultural Research Service), Agricul. Handbook No 60, (1957).

[27] Schwarzenbach, G., Complexometric titrations, Methuen and Co., UK, 45, (1957), pp. 10.

[28] Kuzmann, E., Singh, L.H., Garg, V.K., Oliveira, de A.C., Kovács, E. M., Molnár, Á.M., Homonnay, Z., Kónya, P., Nagy, M. N., and Kónya, J., Mössbauer study of the effect of rare earth substitution into montmorillonite, Hyperfine Interact. 237:(1) (2016) 1-8.

[29] **Kuzmann E, Garg VK, Singh H, de Oliveira AC, Pati SS, Homonnay Z, Rudolf M, Molnár ÁM, Kovács EM, Baranyai E, Kubuki S, Nagy NM, Kónya J., Mössbauer study of pH dependence of iron-intercalation in montmorillonite, Hyperfine Interact. 237:(1) Paper 106. (2016)**

6. LEGENDS TO TABLES AND FIGURES

Figure 1. SEM-EDX spectrum of La-bentonite

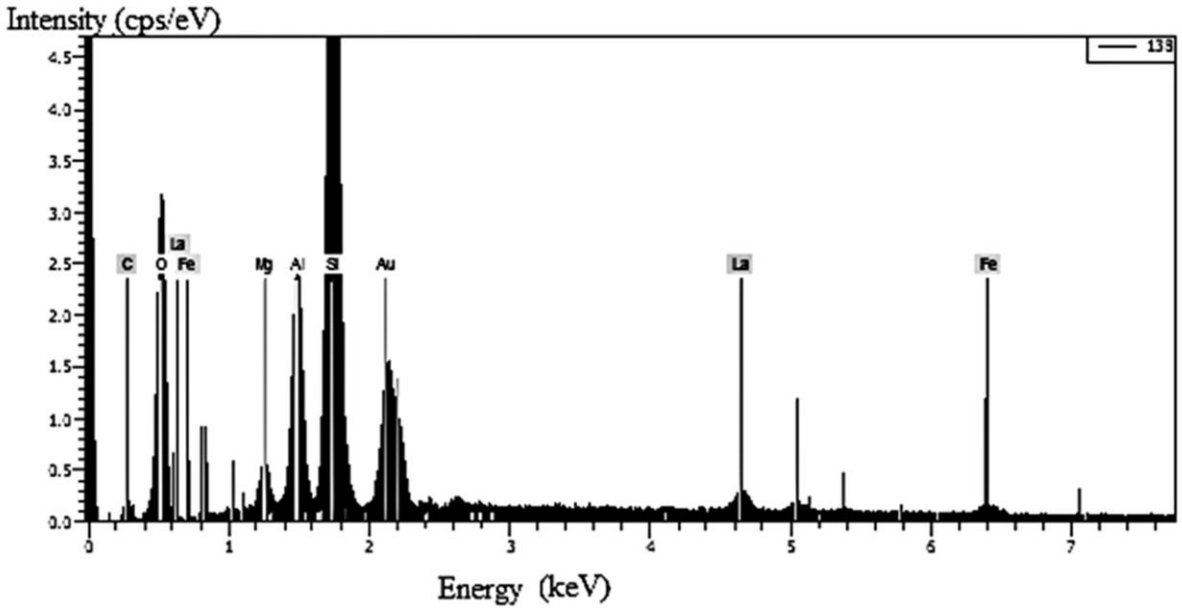

Figure 2. SEM-EDX distribution map of Lu-bentonite

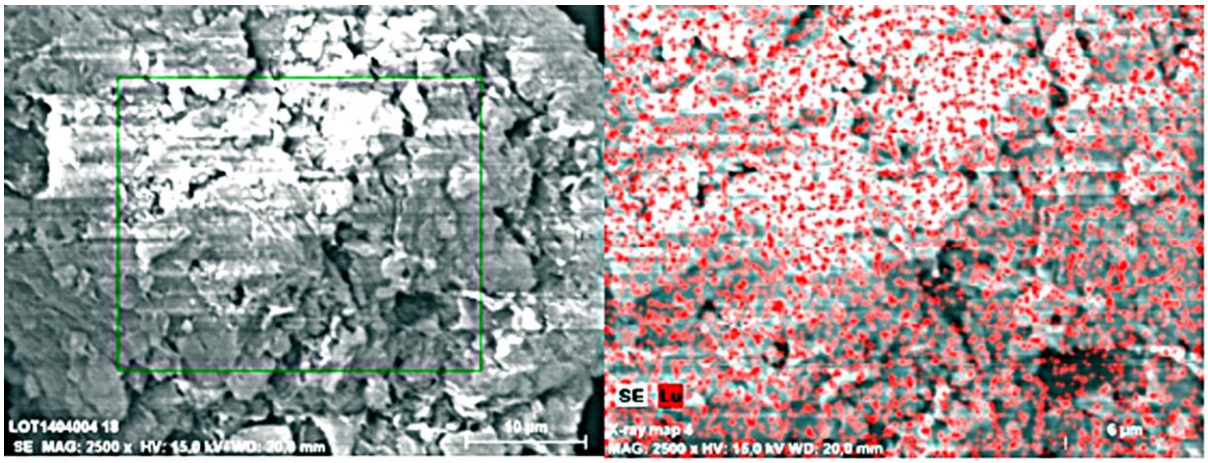

Figure 3. XRD patterns of original Ca-bentonite and some (La, Ce, Gd, Ho) **lanthanide** bentonites

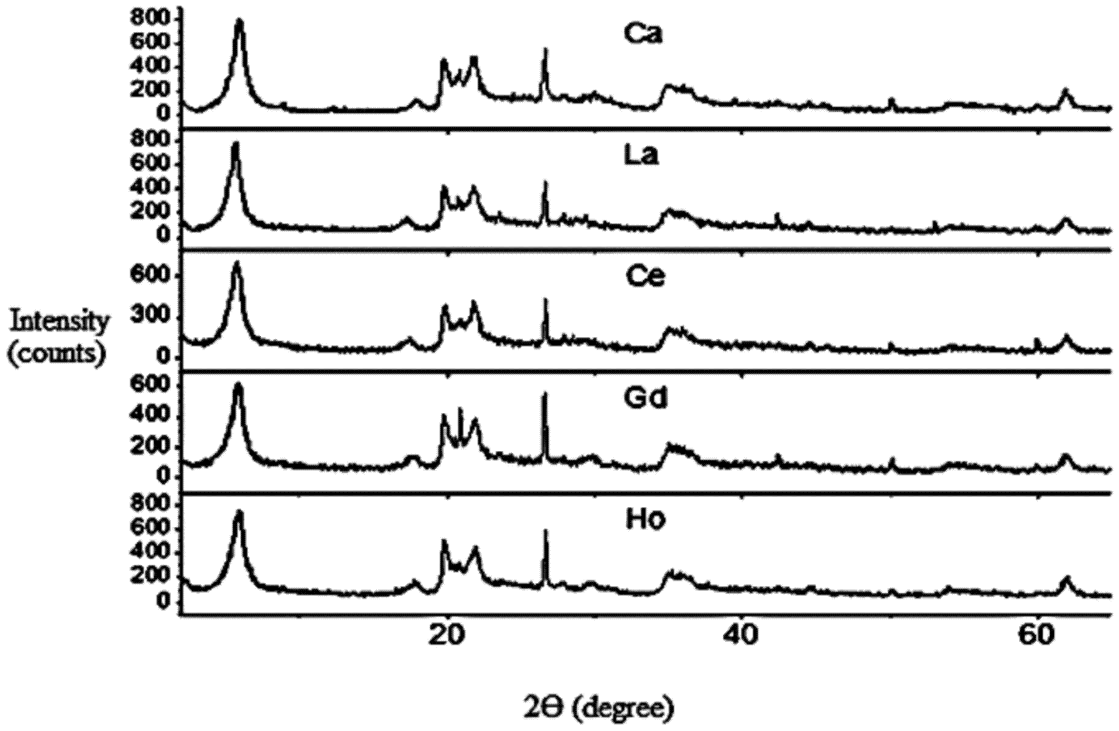

Figure 4. The increase of d_{001} basal spacing of **lanthanide** montmorillonites compared to the Ca-montmorillonite

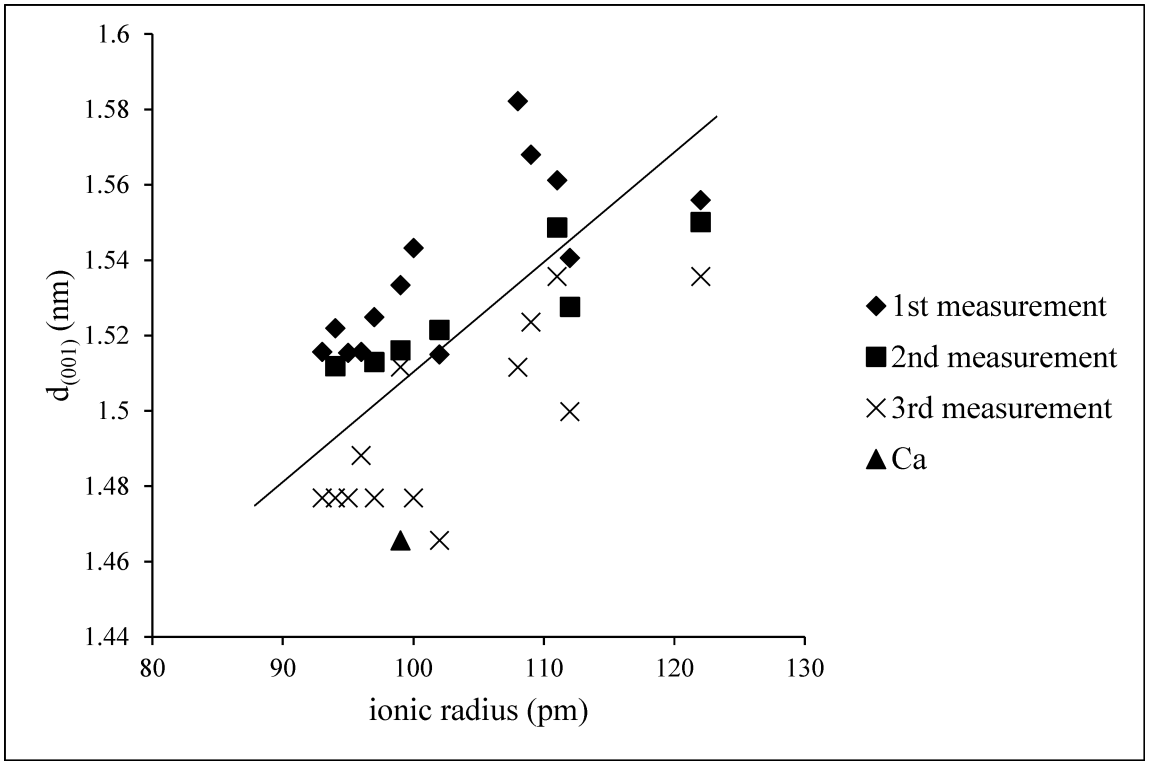

Figure 5. The ^{57}Fe Mössbauer spectra of Ca-bentonite (on the right) and La-bentonite (on the left) measured at 78K

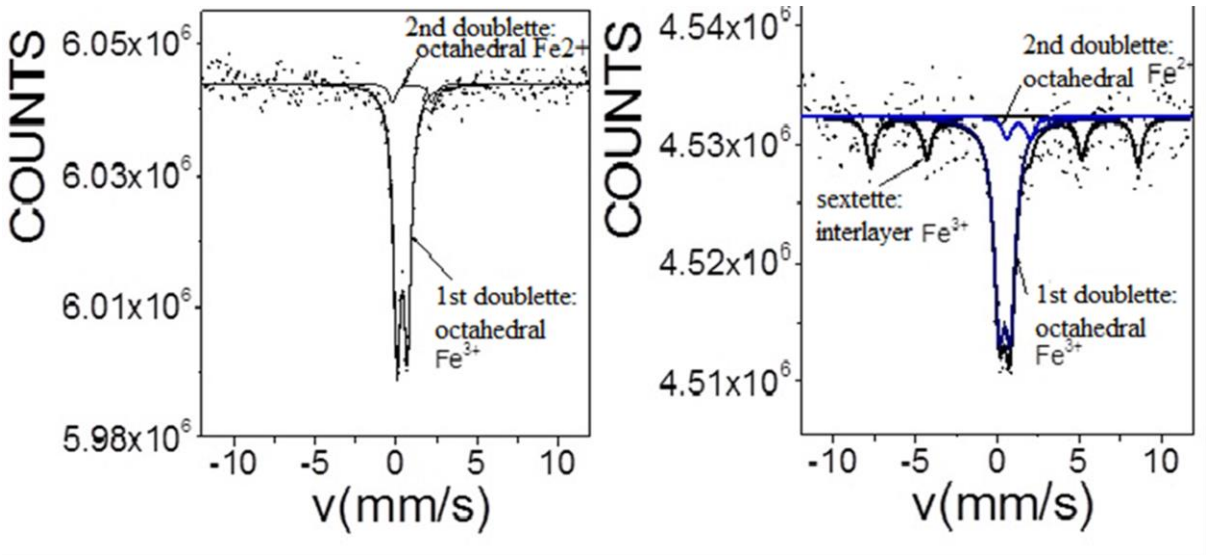

Table 1. Comprehensive table of the last 10 years' literature on modified bentonites

Who, When	Clay	Experimental	Methods	Conclusion
Coppin *et al.*, 2002	Kaolinite, Na-montmorillonite	Lantanoids sorption	XRF- LOI[1], ICP-MS[2], X-ray diffraction (XRD)	The HREEs[3] being more strongly sorbed than LREEs[3].
Tertre *et al.*, 2006	Kaolinite, Na-montmorillonite	Eu^{3+} sorption	TRLFS[4], DLM (diffus layer modell)	An outer-sphere complex is dominant under acidic conditions-> be exchanged with the interlayer cations of the clay mineral. In the other hand an inner-sphere complex, is predominant at higher pH-> bound onto the edges of the particles.
Wu *et al*., 2012	Magnetic Gaomiaozi (GMZ)-Bentonite-> Na-montmorillonite	La^{3+}, Eu^{3+}, Yb^{3+} sorption	Complexometric titration, wide X-ray diffraction (WXRD), FTIR[5], scanning electron microscopy (SEM), zeta potential, N_2 adsorption–desorption isotherms, Magnetization measurement	The magnetic nanocomposite is less efficient than the original bentonite in removing lanthanide ions.
Evgeny *et al*., 2012	FEBEX and MX80 bentonites	Mixed La-Lu sorption	Batch sorption and desorption, XRD, SEM-EDX[6], ICP-OES[7], Langmuir-model	With higher Ln^{3+} concentration, the positive effect on the increase in the lanthanide sorption was overcome by the smectite degradation induced by the presence of Fe.
Stefani *et al*., 2014	Ca-montmorillonite-> La-montmorillonite	Stability on high pressure (HP) and on high temperature (HT)	XRD, SEM-EDX, FTIR	The La-smectite is stable at HPHT, and the structure becomes La-muscovite-like.

[1] XRF-LOI: X-ray fluoresscense spectrometry with loss-on-ignition correction
[2] ICP-MS: Inductively coupled plasma- mass spectrometry
[3] HREE, LREE: Heavy-, low rare earth elements
[4] TRLFS: Time-resolved laser-induced fluorescence spectroscopy
[5] FTIR: Fourier transform infrared spectroscopy
[6] SEM-EDX: Scanning electron microscopy - energy dispersive x-ray specroscopy
[7] ICP-OES: Inductively coupled plasma-optical emission spectrometry

Table 2. Ca^{2+} ion concentration after ion exchange procedure in the solid phase

The exchangeable Ca^{2+} ion concentration on Ca-bentonite (starting material)	8.10E-04	mol/2g	**Ca content related to the exchangeable Ca (%) of the starting material (Ca-bentonite)**
Ca^{2+} ion concentration after 1st exchange on bentonite	6.24E-05	mol/2g	7.7
Ca^{2+} ion concentration after 2nd exchange on bentonite	4.91E-06	mol/2g	0.6
Ca^{2+} ion concentration after 3rd exchange on bentonite	4.10E-07	mol/2g	0.05

Table 3. **Ln**$^{3+}$-ions concentration on bentonites

Ln^{3+}-ions	Initial **Ln**ClO_4 concentrations [mol/dm^3]	Temperature of preparations, (°C)	**Ln** concentrations [mol/g]	**Ln** content related to CEC, (%)
La	0.2	0	3.5E-04	131
	0.2	10	3.6E-04	133
	0.1	25	2.9E-04	107
	0.1		2.7E-04	100
	0.2		3.6E-04	134
	0.2	30	3.7E-04	135
	0.2	40	3.8E-04	136
Ce	0.1	25	2.9E-04	106
Pr	0.1	25	2.7E-04	101
	0.1		2.2E-04	81.5
	0.1		1.9E-04	68.9
Nd	0.1	25	2.8E-04	102
	0.1		2.5E-04	93
Sm	0.1	25	2.5E-04	93.7
Eu	0.1	25	2.9E-04	106
	0.2		3.4E-04	126
Gd	0.1	25	3.1E-04	115
	0.1		3.1E-04	116
	0.1		2.4E-04	87.4
Tb	0.1	25	2.2E-04	83
Dy	0.1	25	3.1E-04	113
	0.1		2.6E-04	94.8
Ho	0.1	25	2.8E-04	104
Er	0.1	25	2.1E-04	77.4
Tm	0.1	25	2.1E-04	79.3
Yb	0.1	25	2.9E-04	107
Lu	0.1	25	2.3E-04	83.7

Table 4. The amount of La, and Fe concentration in case of 200 mg of raw, and modified materials

	La	Fe
	mol/200mg	
Ca-bentonite (starting material)	-	8.1E-05
La exchanged bentonite (1) prepared with 0.2 M initial solution and at 25°C	7.2E-05	3.5E-05
La exchanged bentonite (2) prepared with 0.1 M initial solution and at 25°C	5.6E-05	1.6E-05

Table 5. **Lanthanide** concentration of bentonites, measured by SEM-EDX and XRF

	Ln concentrations [mol/g]	
Lanthanide-bentonite	XRF	SEM
La-bentonite	2.9×10^{-4}	3.0×10^{-4}
Ce-bentonite	2.8×10^{-4}	3.1×10^{-4}
Gd-bentonite	3.1×10^{-4}	2.7×10^{-4}
Lu-bentonite	2.2×10^{-4}	2.1×10^{-4}

Table 6. The amount of Fe, and La concentraion in solid and liquid phase after washing by ammonium acetate

	Fe			La		
	solid	liquid	∑solid, liquid	solid	liquid	∑solid, liquid
	mol/200mg	mol/20ml		mol/200mg	mol/20ml	
Ca-bentonite (starting material)	7.4E-05	9.6E-07	7.5E-05	–	–	–
La exchanged bentonite (1) prepared with 0.2 M initial solution and at 25°C	3.5E-05	1.4E-08	3.5E-05	5.1E-07	7.6E-05	7.6E-05
La exchanged bentonite (2) prepared with 0.1 M initial solution and at 25°C	1.6E-05	<LOD	1.6E-05	5.2E-07	5.0E-05	5.0E-05

Table 7. The amount of Fe concentration, after washing the La-bentonite by ammonium acetate, in solid phase, liquid phase, and washed up from sample holders

	Fe			
	solid	liquid	Washed up from sample holder	∑ solid, liquid, washed up from sample holder
	mol/200mg	mol/20ml	mol/20ml	mol/20ml
La exchanged bentonite (1) prepared with 0.2 M initial solution and at 25°C	3.5E-05	1.4E-08	4.6E-05	8.0E-05
La exchanged bentonite (2) prepared with 0.1 M initial solution and at 25°C	1.6E-05	<LOD	7.01E-05	8.6E-05